Effect of Operation Pressure on the Response of ePNC Particle Number Concentration Sensor

Elmeri Laakkonen, Anssi Arffman, Antti Rostedt, and Jorma Keskinen

***Abstract*—In this article, we present a method that aims toward an ideal number concentration response of a diffusion charger and diffusion collector-based particle sensor (Dekati ePNC) by using reduced pressure conditions in the sensor. A model is derived for the charger and diffusion collector stage of the sensor, as well as for the total particle number concentration (PNC) response. The derived model is validated with experimental characterization measurements in different operation pressures. The experimental results show that reduced operation pressure makes the sensor response less dependent on particle size, approaching pure particle number response. The obtained results improve the feasibility of the diffusion charging-based method in the measurement of PNC.**

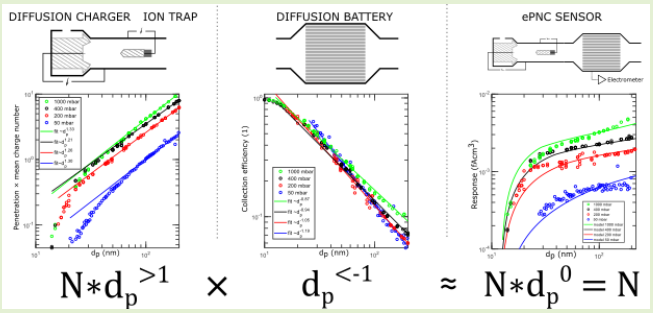

***Index Terms*— Aerosols, air pollution, air quality, diffusion battery (DB), diffusion charger, effect of pressure, environmental monitoring, nanoparticles, particle charging, particle measurements.**

I. Introduction

AMBIENT aerosol particles, especially fine particles (PM2.5, particles smaller than 2.5 μm in diameter) are estimated to cause several million premature deaths annually [1]. Although research has hitherto failed to identify the aerosol components behind the toxicity, there is nevertheless increasing evidence of the short-term effects of ultrafine particles (UFP), particles smaller than 100 nm [2]. This has motivated the WHO to recommend quantifying the UFP in terms of particle number concentration (PNC) in the latest air quality guidelines [3]. Meanwhile, solid particle number (SPN) was introduced as a metric for automotive emission measurement [4] and integrated into the European emission legislation in 2009.

Condensation particle counter (CPC) has been the instrument of choice for PNC measurement [5], [6]. The CPC offers a practically zero-background particle count with a well-defined lowest measured particle diameter. There is, however, a need for less expensive and more robust instruments in various monitoring applications, such as air quality, vehicle emissions—including portable emission measurement (PEMS)— and vehicle periodic technical inspection (PTI). The unipolar diffusion charging (DC) principle offers the possibility to develop simple, low-cost, and robust monitoring instruments [7]. DC-based instruments have been successfully applied to solid particle measurement in PEMS [8]. Later studies by Melas et al. [9] have shown that in addition to the PEMS, the DC-based instruments are able to meet the requirements related to vehicle PTI.

One of the first simplified DC-based instruments for vehicle emission measurement was presented by Ntziachristos et al. [10]. This instrument combined a diffusion charger, a precut impactor, and a Faraday cage filter. The output of the instrument was demonstrated to closely follow the total active surface area of the particles. Later, Rostedt et al. [11] presented a DC-based sensor-type instrument for the particle emission measurement, consisting of a probe placed directly in the exhaust flow. An approximation of the mean particle diameter was required in converting the measured signal to mass or number concentration.

Amanatidis et al. [12] presented the first approach to measure the number concentration in vehicle exhaust in real time with sensor-type instruments. This approach used two Pegasor PPS-M sensors operated with different operation parameters to obtain particle number and mass concentration together with the mean particle size. Schriefl et al. [13] presented a sensor-type instrument design where measurement output

Manuscript received 25 September 2023; accepted 17 October 2023. Date of publication 20 November 2023; date of current version 2 January 2024. This work was supported in part by Dekati Ltd., Kangasala, Finland; and in part by the Tampere University Aerosol Measurement Infrastructure, through the Academy of Finland Infrastructure Funding under Grant 337225. The associate editor coordinating the review of this article and approving it for publication was Dr. Ponnalagu R. N. *(Corresponding author: Antti Rostedt.)*

Elmeri Laakkonen is with Dekati Ltd., 36240 Kangasala, Finland and Aerosol Physics Laboratory, Tampere University, 33720 Tampere, Finland.

Anssi Arffman is with Dekati Ltd., 36240 Kangasala, Finland.

Antti Rostedt and Jorma Keskinen are with the Aerosol Physics Laboratory, Tampere University, 33720 Tampere, Finland (e-mail: antti.rostedt@tuni.fi).

Digital Object Identifier 10.1109/JSEN.2023.3329519

follows the PNC of the exhaust gas. This design is based on the combination of a particle DC and an electrostatic precipitator. It was demonstrated that the signal measured from the instrument followed the PNC in the particle size range relevant to the exhaust emission measurement.

Recently, a DC-based particle number sensor (ePNC, manufactured by Dekati Ltd.) was introduced, combining a diffusion charger and a diffusion battery (DB) in a series configuration. Karjalainen et al. [14] used the ePNC sensor in the SPN measurement to study the operation of auxiliary heaters of passenger cars and compared the results with other methods. The ePNC sensor-based PEMS system was featured in recent PTI sensor studies by Melas et al. [15] and Vasilatou et al. [16] with different particle materials and morphology.

In the ePNC sensor, the current is measured from the DB, which collects only a fraction of all particles passing through the DB. Both the charger and the DB are operated at a reduced pressure both to modify the sensor response and to decrease the partial pressure of condensable species. In this article, we study both experimentally and theoretically the effect of pressure on the responses of the charger and collector components of the sensor; furthermore, we analyze how the lowered pressure can be applied to improve the overall number concentration response of the sensor.

II. Methods

A. Sensor Operation Principle and PNC Response

In general, the response of an aerosol diffusion charger is proportional to a power function of particle diameter ($\propto d_p^b$), with the exponent b between one and two. Because of this, some additional measures are required in order to be able to measure the number concentration with a DC-based sensor. It is possible to incorporate a simplified mean particle size measurement using an electrostatic precipitator as a simple mobility analyzer [17] or a DB [18]. With this information, the DC-based signal can be converted to number concentration. An appealing alternative is to directly modify the instrument response by combining the charger with a collector having a response as closely as possible proportional to particle diameter to the power of $-b$ ($\propto d_p^{-b}$). This was accomplished by Schriefl et al. [13], effectively measuring only the fraction of diffusion-charged particles collected by a electrostatic precipitator. The ePNC sensor is based on an analogous concept of measuring only the fraction of diffusion charged particles collected by a DB.

A schematic view of the sensor studied in this article is shown in Fig. 1. The sensor is composed of a needle-cylinder geometry corona discharge diffusion charger followed by an electrostatic collector serving as an ion trap, and finally, a circular tube bundle DB connected to an electrometer for current measurement. A characteristic feature of the sensor is the use of a critical orifice at the inlet to decrease the operation pressure. This serves to reduce the partial pressure of condensing species below the saturation pressure without the need for extra heating or dilution systems; however, the operation pressure also affects the response functions of both the charger and the DB. In this section, theoretical response models for the components are presented, enabling the analysis of the effect of pressure on the instrument's overall response.

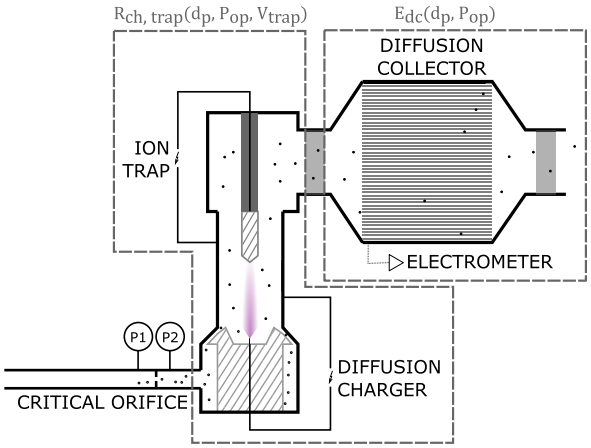

Fig. 1. Schematic view of the ePNC sensor.

The primary components affecting the overall response of the sensor are the charger response R_{ch}, ion trap penetration P_{trap} and diffusion collector collection efficiency E_{dc}. The combined sensor number concentration response R is a function of the particle size d_p, operating pressure P_{op} and the voltage of the ion trap V_{trap}. The overall sensor response R can be expressed as follows:

$$\begin{aligned}\frac{I_{\text{sensor}}}{N} &= R\left(d_p, P_{\text{op}}, V_{\text{trap}}\right) \\ &= R_{\text{ch}}\left(d_p, P_{\text{op}}\right) P_{\text{trap}}\left(d_p, P_{\text{op}}, V_{\text{trap}}\right) E_{\text{dc}}\left(d_p, P_{\text{op}}\right)\end{aligned} \tag{1}$$

where I_{sensor} is the current measured by the sensor and N is the input number concentration. Combining the charger response R_{ch} and ion trap penetration as total charger response $R_{\text{ch,trap}}$ (1) can be simplified as follows:

$$R\left(d_p, P_{\text{op}}, V_{\text{trap}}\right) = R_{\text{ch,trap}}\left(d_p, P_{\text{op}}, V_{\text{trap}}\right) E_{\text{dc}}\left(d_p, P_{\text{op}}\right). \tag{2}$$

In the ideal case of a number concentration measuring sensor, the product of charger response and the collection efficiency should, therefore, be independent of the particle size to have a one-to-one relation between the measured current and number concentration.

B. Theoretical Response Model

The flow through the ePNC device is controlled by a critical orifice, which defines the mass flow rate through the device under constant ambient conditions. Under constant mass flow rate assumption, the volumetric flow rate is inversely proportional to the pressure, and therefore, variable with pressure conditioning of the device. The flow rate affects residence time of particles in all components of the device, and therefore, pressure is a critical factor in modeling of the sensor response, as particle losses by different mechanisms such as diffusion are dependent on the residence time.

The average charge per particle produced by the corona charger was modeled using the charging model presented, e.g., in Hinds [19]. The model gives separate expressions for the ion diffusion and electric field charging phenomenon and by adding both charging terms the combined charging level can

TABLE I
VALUES AND SYMBOLS USED IN THE CHARGER MODEL

Parameter	Symbol	Value	Unit
Air viscosity	η_{air}	$1.8 \cdot 10^{-5}$	Pa s
Molecular mass	M_{air}	0.0289	kg/mol
Real gas constant	R	8.315	J/K/ mol
Boltzmann constant	k	$1.38 \cdot 10^{-23}$	J/K
Elementary charge	e	$1.6 \cdot 10^{-19}$	C
Electrostatic constant	K_E	$9 \cdot 10^9$	Nm^2/C^2
Mean thermal speed of ion	c_i	240	m/s
Corona current	I_{ch}	1	µA
Charger residence time	t_{ch}	$3/12/24/60 \cdot 10^{-3}$	s
Charger surface area	A_{ch}	$4.14 \cdot 10^{-4}$	m^2
Ion electrical mobility (STP)	Z_0	$1.5 \cdot 10^{-4}$	$m^2/V/s$
Particle relative permittivity	ϵ	3	1
Trap voltage	V_{trap}	10.5 or 110	V
Trap inner diameter	R_i	6	mm
Trap outer diameter	R_o	12	mm
Trap length	L	20	mm
Inlet flow rate	Q	1.81	slpm
Fitted ion density (1000 mbar)	N_i	$9 \cdot 10^{14}$	$\#/cm^3$

be estimated. The model equations were

$$n_{\text{diff}}(t) = \frac{d_p kT}{2K_E e^2} \ln\left(1 + \frac{\pi K_E d_p c_i e^2 N_i t}{2kT}\right) \tag{3}$$

and

$$n_{\text{field}}(t) = \left(\frac{3\epsilon}{\epsilon + 2}\right)\left(\frac{E d_p^2}{4K_E e}\right)\left(\frac{\pi K_E e Z_i N_i t}{1 + \pi K_E e Z_i N_i t}\right) \tag{4}$$

where d_p is the particle size, k the Boltzmann's constant, T the absolute temperature, K_E the Coulombic repulsion-related constant, c_i the mean thermal speed of ions, N_i the ion concentration, t the residence time in the ion cloud, ϵ the relative permittivity of the particle material, E the electric field strength, Z_i the ion mobility, e the elementary charge. Table I shows the values of the constants and parameters used in the model.

The residence time, ion mobility, and ion concentration are variables influenced by the gas pressure. The average residence time is obtained simply by dividing the charger volume by the volumetric flow rate $t = V_{\text{ch}}/Q_{\text{vol}}$. Keeping the mass flow rate constant, the volumetric flow rate is increased with reduced pressure, making the residence time directly proportional to the pressure ($t \propto P$). As discussed by, e.g., Mason and McDaniels [20], the ion mobility is inversely proportional to the number density of the gas molecules. We can, therefore, write $Z_i = Z_0(P_0/P)$, where Z_0 and P_0 are the ion mobility and gas pressure in reference conditions, and P is the actual gas pressure surrounding the ion.

For the ion concentration, in a current-limited needle-cylinder type corona charger, one can derive a simple expression by applying the charge conservation principle

$$N_i = \frac{I_{\text{ch}}}{e A_{\text{ch}} v_i} \tag{5}$$

where I_{ch} is the charger current and A_{ch} the charger ground plate surface area. The velocity of ions depends on the pressure through the ion mobility, giving

$$v_i = E Z_i = E Z_0 \frac{P_0}{P}. \tag{6}$$

This does not take into account any possible changes in ion composition as a function of the pressure. The electrical force is offset by the gas friction, and the ion velocity is inversely proportional to gas pressure it is traveling. Peek's law for thin wires describes the visual corona discharge onset electric field strength and the empirical expression found by Peek [21]

$$E_p = E_R \delta_R \left(1 + \frac{k_R}{\sqrt{r \delta_R}}\right) \tag{7}$$

where E_R and k_R are constants with values of $3.1 \cdot 10^6$ V/m and 0.0308 $m^{1/2}$, respectively, and $\delta_R = P/T$. If the E_p is plotted as a function of P for $r = 50$ μm one finds

$$E_p \propto \sqrt{P}. \tag{8}$$

If this is inserted into (6) and the result is further inserted into (5) the ion density can be found to be dependent on charger pressure accordingly

$$N_i \propto \sqrt{P}. \tag{9}$$

The product of ion density and residence time $N_i t$ is another commonly used measure of diffusion chargers. The pressure dependency of $N_i t$ is

$$N_i t \propto P^{\frac{3}{2}}. \tag{10}$$

The residence time also affects the performance of the ion trap making the whole charger system dependence on pressure slightly more complicated. The ion density N_i was used in the model as a fitting parameter following the pressure dependence given by (9).

The effect of ion trap on the particle penetration through the charger was modeled as an annular laminar flow cylindrical mobility analyzer with inner radius R_{in}, outer radius R_{out} and length L. The limiting electrical mobility is given by

$$Z_0(V_{\text{trap}}) = \frac{Q \ln\left(\frac{R_{\text{out}}}{R_{\text{in}}}\right)}{2\pi V_{\text{trap}} L} \tag{11}$$

where Q is the volumetric flow rate through the charger and V_{trap} is the applied voltage. The trap voltages used were chosen near the minimum and maximum voltages of the sensor for the maximal magnitude of the effect. The limiting electrical mobility calculated by (11) is assumed to be valid within this range. The collection efficiency of the trap is

$$E(Z_p) = \frac{Z_p}{Z_0} \tag{12}$$

where Z_p is the electrical mobility of particles. The average charge in the calculation of Z_p was calculated according to (3) and (4) except when the average charge falls below unity the particle charge was assumed to be 1 elementary charge. Diffusion and inertial losses also contribute to the penetration of the charger, but these effects were neglected in the current model. Parameter values used in the charger response modeling are collected in Table I.

Equation (3) describing the DC process is expected to be accurate within a factor of 2 for the studied particle size range at atmospheric pressure [19]. Lower pressures decrease $N_i t$-values, narrowing the accurate particle diameter range. One should note that there is a relatively large uncertainty

already in the pressure scaling of the $N_i t$-values. In the end, the theoretical equations are applied to help in estimating the trends in the overall response function of the instrument, not to predict the exact particle charge.

The structure of the implemented diffusion collector is similar to that of a common catalytic converter comprising multiple circular parallel channels of the same length. Reynolds number of flow in a single channel is below 1, and therefore, the flow in a channel is laminar.

Gormley and Kennedy [22] derived an analytical expression for the diffusional deposition of particles from a laminar tube flow, which can be used to model the diffusion collector of the sensor. The transport efficiency is a derived as a function of dimensionless term h, which depends on the particle diffusion coefficient D, the tube length L and volumetric flow through the tube Q

$$h = \pi \frac{DL}{2Q}. \tag{13}$$

According to Gormley and Kennedy [22], the particle transport efficiency in laminar tube flow for particles affected by diffusional deposition can be approximated by

$$P_{\text{tube,diff}} = \begin{cases} 1 - 4.036h^{2/3} + 2.4h + 0.446h^{4/3}, & h < 0.0156 \\ 0.8191e^{-7.314h} + 0.0975e^{-44.6h} + 0.0325e^{-114h}, & h \geq 0.0156. \end{cases} \tag{14}$$

Approximating the collector as multiple parallel tubes of same length and diameter the particle collection efficiency of the diffusion collector E_{diff} is given by

$$E_{\text{diff}} = 1 - P_{\text{tube,diff}} \tag{15}$$

where $P_{\text{tube,diff}}$ is the particle transport efficiency of a single diffusion collector channel.

The diffusion coefficient for a particle of diameter d_p can be expressed as

$$D = \frac{k_B T C_C}{3\pi \eta d_p} \tag{16}$$

where k_B is the Boltzmann's constant, T is the temperature, C_C is Cunningham's slip correction factor, η is the dynamic viscosity of the gas. The slip correction factor is dependent on the free path of gas molecules, which is inversely proportional to pressure [23].

The dimensionless term h includes pressure-dependent terms diffusion coefficient D and volumetric flow rate Q. The flow through the ePNC device is controlled by a critical orifice, which defines the mass flow rate through the device under constant ambient conditions. Under the constant mass flow rate assumption, the volumetric flow rate is inversely proportional to the pressure. The collection efficiency for different operation pressures is shown in Fig. 2(c). The parameters and their values used in the diffusion collection model are shown in Table II.

Fig. 2(c) shows that the collection efficiency is roughly proportional to $a \cdot d_p^b$ at particle size range 20–200 nm where a and b are fit constants. Comparing the collection efficiencies in different operation pressures shows the possibility of varying the exponential dependency of collection efficiency by modifying the operation pressure of the diffusion collector. The reduced pressure conditions shown in Fig. 2(c) result in lower exponent b values.

TABLE II
VALUES AND SYMBOLS USED IN THE DIFFUSION COLLECTOR MODEL

Parameter	Symbol	Value	Unit
Air viscosity	η_{air}	$1.8 \cdot 10^{-5}$	Pa s
Channel length	L	0.15	m
Mass flow rate per collector channel[1]	Q	$0.83 \cdot 10^{-3}$	slpm

[1]The mass flow rate was scaled to volumetric flow in the sensor pressures accordingly.

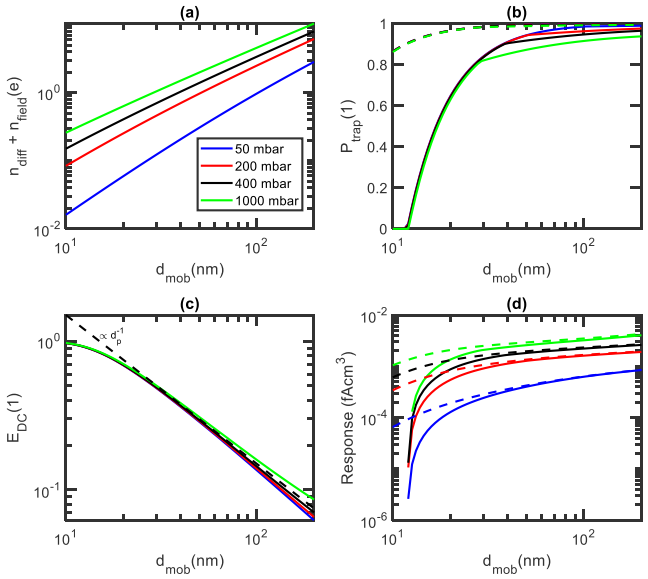

Fig. 2. (a) Average charge of particles predicted by the combined diffusion and field charge model, (b) penetration of the trap after the charger (solid lines 110 V and dashed lines 10 V trap voltage), (c) diffusion collector collection efficiency, and (d) product of the charger response and diffusion collector collection efficiency for different operation pressures.

The overall sensor number concentration response is the product of charger response and diffusion collection efficiency, as shown in (2). Fig. 2(c) shows that under reduced pressure conditions the exponent b value is roughly of order $-0.85, \ldots, -1.1$ (pressure range 50–1000 mbar), which can be used to compensate for the particle size dependence of a unipolar diffusion charger correspondingly in the power function exponent range of $0.85, \ldots, 1.1$.

Fig. 2 shows the modeled response components and total response as a function of particle size in different operating pressures and different trap voltages. The total response is calculated as a product of charger response—including the trap penetration efficiency—and diffusion collector collection efficiency. The field charging term is small compared to the DC term in the plot of Fig. 2(a) but the total charger response efficiency is shown here. Tables I and II show the parameters and their values used to model the charger and the diffusion collector.

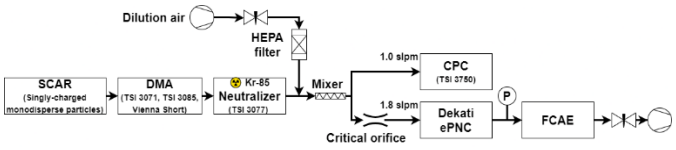

Fig. 3. Measurement setup used in the sensor response characterization measurements.

III. Experimental

The objective of experimental measurements was to validate the obtained model and evaluate the PNC response of the sensor and explore the effect of different operating pressures to the overall response. Before measurements the electrical calibration of ePNC electrometer was verified against a calibrated reference current source.

Two custom-built aerosol generators based on the Single Charged Aerosol Reference (SCAR) [24] were used as the generators during the response calibration measurements. In SCAR, small, single-charged seed particles (produced by evaporation-condensation with tube furnace and dilution; NaCl and Ag were used) were grown by dioctyl sebacate (DEHS) condensation, resulting in nearly monodisperse aerosol with each particle having only one elemental charge. Generated particle morphology was assumed to be spherical. The generated aerosol was classified using various differential mobility analyzers (DMAs), resulting in a truly monodisperse single-charged sample aerosol. Externally monitored closed recirculating sheath flow control was used with all DMAs. The classified monodisperse sample was then neutralized using an ^{85}Kr aerosol neutralizer (TSI, Model 3077) to minimize the effect of the initial charge state of the particles. Additional dilution with particle-free air was used to adjust the flow rate of the DMA and to supply enough samples for the measurement devices. ePNC (Dekati Ltd.) and CPC (TSI Model 3750, two different units were used) sampled the aerosol in parallel. The CPC was used as a PNC reference instrument. A Faraday cup aerosol electrometer was installed in the line after ePNC, collecting the fraction of particles that were not deposited in the diffusion collector. Using the additional Faraday cup aerosol electrometer after the sensor allows for separate measurements of the diffusion collection efficiency and the charger response. A single critical orifice corresponding to a 1.8 slpm flow rate was used in all measurements to keep the sample flow rate similar in all circumstances. A digital pressure gauge (Druck DPI 104) was used to monitor the pressure after the ePNC. Pressure losses in the charger and DB of the sensor are negligible compared to the critical orifice, and therefore, the measured pressure is indicative of the pressure inside of the sensor. A schematic of the measurement setup is shown in Fig. 3. The particle fraction collected by the Faraday cup aerosol electrometer after ePNC is charged by the charger integrated into the ePNC sensor and is then measured by another electrometer. Assuming net charge state of the introduced particles being neutral and the losses between ePNC and FCAE being negligible the total current due to ePNC charger response is given by the sum of current measured by the sensor and the current measured by the FCAE. The charger response is, therefore, given by

$$R_{\mathrm{ch,trap}}\left(d_p, P_{\mathrm{op}}, V_{\mathrm{trap}}\right) = \frac{I_{\mathrm{sensor}} + I_{\mathrm{FCAE}}}{N} \tag{17}$$

where N is the number concentration measured by the reference CPC at the ambient pressure.

We introduce here one more quantity to describe the charger response, the Pn-product [25]

$$Pn = \frac{I_{\mathrm{sensor}} + I_{\mathrm{FCAE}}}{NeQ_n} = \frac{R_{\mathrm{ch,trap}}\left(d_p, P_{\mathrm{op}}, V_{\mathrm{trap}}\right)}{eQ_n}$$

where P is the penetration of particles through the charger and ion trap, n is the average number of elementary charges per particle, and e is the elementary charge. As N is measured at ambient pressure, so is the volumetric flow rate Q_n. Operating with constant mass flow, Q_n has a constant value. The Pn-product is dependent on particle diameter, the operating pressure, and the trap voltage. We use the Pn-product as a separate quantity that can readily be accurately measured [25].

The collection efficiency of the diffusion collector is given by the ratio of current measured by the sensor to the total measured current

$$E_{\mathrm{dc}}\left(d_p, P_{\mathrm{op}}\right) = \frac{I_{\mathrm{sensor}}}{I_{\mathrm{sensor}} + I_{\mathrm{FCAE}}} \tag{18}$$

where I_{sensor} is the current measured by the sensor and I_{FCAE} is the current measured by the Faraday cup aerosol electrometer after ePNC.

The sensor number concentration response is then given as a product of charger response and diffusion collection efficiency. The FCAE-measured current is not needed for the total sensor response calculation

$$\begin{aligned} R\left(d_p, P_{\mathrm{op}}, V_{\mathrm{trap}}\right) &= R_{\mathrm{ch,trap}}\left(d_p, P_{\mathrm{op}}, V_{\mathrm{trap}}\right) E_{\mathrm{dc}}\left(d_p, P_{\mathrm{op}}\right) \\ &= \frac{I_{\mathrm{sensor}} + I_{\mathrm{FCAE}}}{N} \cdot \frac{I_{\mathrm{sensor}}}{I_{\mathrm{sensor}} + I_{\mathrm{FCAE}}} = \frac{I_{\mathrm{sensor}}}{N}. \end{aligned} \tag{19}$$

The sensor response was measured in four different operating pressures (50, 200, 400, and 1000 mbar) using two different ion trap voltages (10 and 110 V) with monodisperse aerosol in the particle size range of 10 to 200 nm. The same charger and collection unit were used in 200, 400, and 1000 mbar measurements, while the 50 mbar measurements were made with a different collector unit. This affects the diffusion collector efficiency, and therefore, the total sensor response when comparing the 50 mbar measurements to other measurements. The mass flow rate through the sensor was 1.8 slpm and converted to the equivalent volumetric flow rate in the lowered pressure conditions, it equals 1.8–36.5 lpm.

IV. Results

A. Charger Response

The measured and modeled charger Pn-values are shown for 110 V trap voltage in Fig. 4(a) and for 10 V trap voltage in Fig. 4(b).

The charger response drops for all particle sizes with reduced pressure due to reduced ion density, as expected

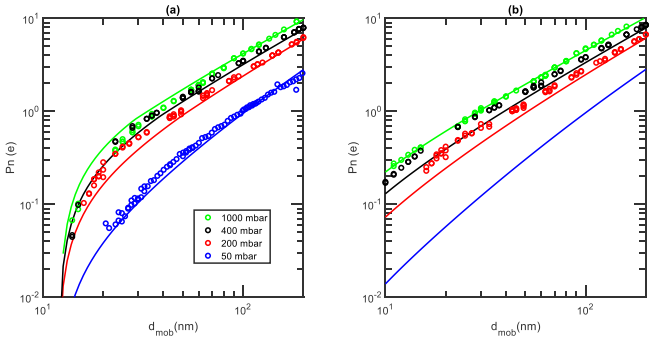

Fig. 4. Measured (dots) and theoretical charger *Pn*-values as a function of particle size at different charger operation pressures. (a) Shows the results for 110 V trap voltage and (b) for 10 V trap voltage.

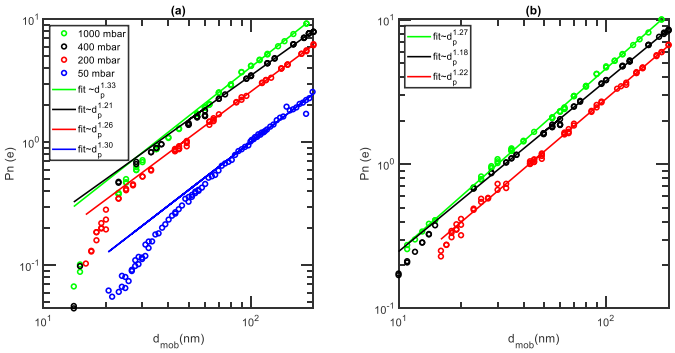

Fig. 5. Measured charger *Pn*-values (dots) and the fits (lines) as a function of particle size at different charger operation pressures. (a) Shows the results for 110 V trap voltage and (b) for 10 V trap voltage. Fittings include only particle sizes above 100 nm.

from the relation given in (9). The 50 mbar measurements were done just to validate the model as the charger response decreases to an undesirably low level. The *Pn*-values with 110 V trap voltage curve down at increasing particle diameters with decreasing pressure. This is caused by increasing collection in the ion trap as particle mobility increases with increasing slip correction factor.

The charger model fits very well with the measured values for particles larger than 100 nm but somewhat underestimates the *Pn*-values for smaller particles at lower pressures. As discussed by Hinds, the lowest particle size correctly estimated by (3) increases for decreasing *Nt*-values, which here means the lowest pressure values [19]. In addition, the deterministic approach breaks down when the calculated charge number per particle goes beyond unity. Nevertheless, the model agrees with the measurements in predicting that the reduced pressure has little effect on the particle size dependence of the charger response.

Fig. 5 shows power law ($a \cdot d_p^b$) fits to measured *Pn*-values. The effect of the ion trap particle collection efficiency on the fit was minimized by fitting the function to only particle sizes larger than 100 nm.

The ion density used in the modeled charger response was fit using the experimental results according to (9). The fit ion density as function of sensor operating pressure is shown in Fig. 6.

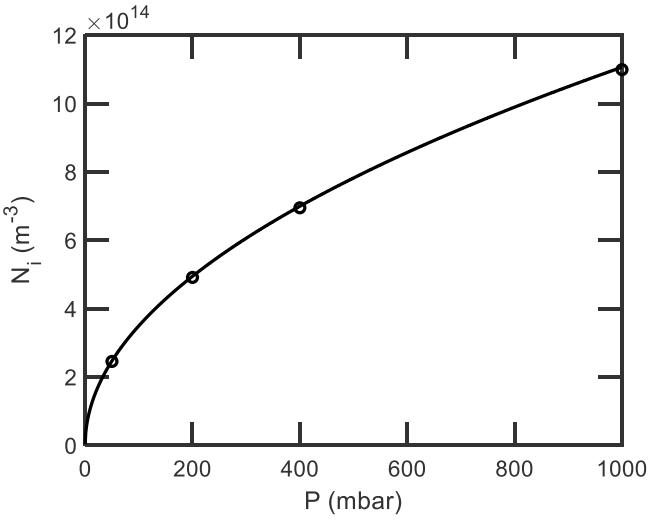

Fig. 6. Fit ion density in the charger as a function of pressure (dots). The solid line shows a fit of the form given by (8). The fit was found to be $N_i = 3.5 \cdot 10^{12}\ P^{1/2}$, where P is expressed in Pascals.

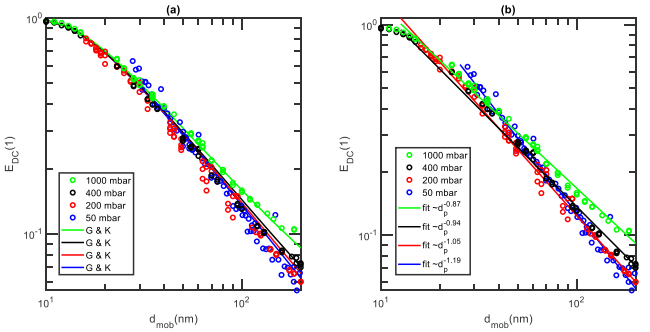

Fig. 7. Diffusion collector collection efficiency in different operation pressures with a constant mass flow rate. (a) Measurement results (dots) and theoretical collection efficiencies (lines) according to Gormley and Kennedy [22] are presented and (b) measurement results and fits of form $a \cdot d_p^b$ to measurements are presented.

B. Diffusion Collector Collection Efficiency

Fig. 7 shows the measured and modeled diffusion collector response. Theoretical diffusion collection efficiency, according to Gormley and Kennedy [22] was fit in the left-hand side of Fig. 7, and a fit of type $a \cdot d_p^b$ is shown on the right-hand side of Fig. 7. The 50 mbar measurements were done with a different collector unit, which explains some of the difference in the slope when compared to other measurements.

Fig. 7 shows that the diffusion collector behaves as expected in different pressure conditions. The change in collection efficiency for particles larger than 100 nm is significant, but for small particles under 30 nm, the effect is not as clear. The change in $a \cdot d_p^b$ fit exponents shown in Fig. 7(b) shows the possibility to use the diffusion collector as a compensator for diffusion chargers with opposite exponents.

C. Overall Sensor Response

Fig. 8 shows the measured and modeled overall sensor response, which is the product of the total charger response and the diffusion collector collection efficiency presented above. The sensor overall response decreases with decreasing

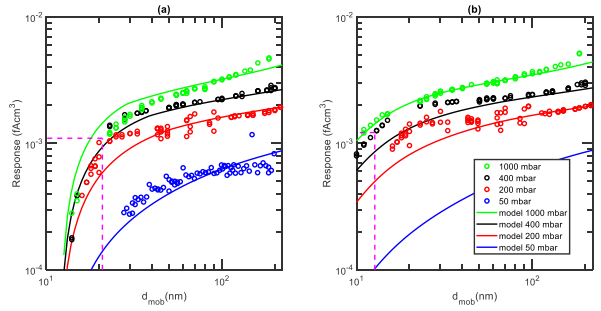

Fig. 8. Measured sensor response [dots, as stated in (2)] and theoretical response (solid lines) in different operation pressures. (a) Trap voltage was 110 V and (b) 10 V. The dashed lines in the figures show the indicative limits for the lowest detectable particle size.

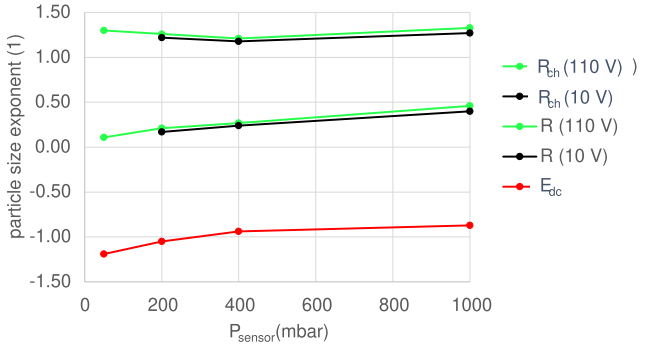

Fig. 9. Particle size dependency of charger, diffusion collector, and the sensor overall response as a function of sensor operation pressure (exponent values from the fits of Figs. 5 and 7).

operation pressure due to the decreased charging efficiency. The trap voltage does not significantly affect the response in the particle sizes above 30 nm but affects the response in smaller sizes. In fact, the trap voltage setting provides the means to tailor the lowest detectable particle size limit of the sensor. This is demonstrated in Fig. 8 by plotting dashed lines to show a 50% response limit compared to the response with 100 nm particle size. This gives indicative values for the lowest detectable particle size of 13 and 21 nm for trap voltages of 10 and 110 V, respectively. These values can be further modified to the application-specific needs by altering the trap voltage setting.

The effect of the operating pressure on the total sensor response was studied as the product of the $a \cdot d_p^b$ fits for charger response and collection efficiency. For an ideal number concentration response, the components would compensate each other perfectly and the sensor response exponential term, which is the sum of components' exponents would be zero. The multiplicative a term is significant only for the sensitivity of the sensor. Fig. 9 shows the exponent terms of fits for charger response, collection efficiency, and the overall response as a function of the sensor operation pressure. The overall sensor response exponent approaches zero with reducing pressure, making the sensor response more independent of particle size at lower pressure conditions.

V. Discussion

As mentioned above, the low particle diameter and the low-pressure combination is, in principle, beyond the validity range of the charging model, but it still successfully describes the general trend of the charger response in reduced pressure conditions. The diffusion model presented by Gormley and Kennedy [22] was found to be adequate in describing the diffusional collection of particles in the collector in reduced pressure conditions. The modeled effect of pressure on the overall sensor response was also found to be similar to that of measured.

Reduced pressure conditions inside the sensor prevent the condensation efficiently. The 400 mbar operation pressure was found to be a good practical operation point for the sensor. This allows the use of a critical orifice for flow control while still having a high response and a relatively flat number concentration response. Given the mass flow rate of the sensor, 400 mbar is within the reach of inexpensive diaphragm gas pumps, while even lower pressure would likely require a larger pump or lower flow rate.

In addition to operating the charger and diffusion collector at the same pressure, the derived model allows to study the response when operating the charger and the collector at different pressures. This approach would be beneficial for increased sensitivity because it allows the use of the charger at ambient pressure conditions to maintain a higher charger response. Critical orifice flow control could be retained by placing the orifice after the charger. The diffusion collector pressure could then be reduced without change in the charge state of the aerosol allowing for additional adjustability of the compensation as function of the collector pressure; however, this method exposes the charger to possible condensation when used in emission applications where the measured exhaust sample may contain large amounts of water vapor.

Both the experiments and the modeling were limited to spherical particles only, neglecting any particle material or morphology-specific effects. DC dominates the charging process for the particle size range studied here, but the relative permittivity of the particle material has some effect on the field charging, as shown in (4). Fractal-like agglomerates, such as soot particles, are known to obtain somewhat higher charge levels in diffusion chargers compared to spherical reference particles of similar mobility size [26], [27]. They might also cause a change in the size dependence of the charger response curve.

VI. Conclusion

The effect of reduced pressure conditions on the response of a diffusion charger and a diffusion collector-based sensor was studied experimentally and by modeling. The particle size dependence of each component was studied by comparing the derived model to experimental results and using power law-type functions fit to describe the particle size dependency in the size range of 10 to 200 nm. According to the experimental and modeling results, reducing the sensor operating pressure can be used to compensate for the increase in charger response at larger particle sizes, making the sensor's number concentration response closer to ideal. The results also make it possible to predict changes in the sensor response when operating the charger and the diffusion collector at different pressures. DC-based instruments are well known for being

simple and sturdy devices. The obtained results improve the feasibility of this method in the measurement of PNC.

REFERENCES

[1] J. Lelieveld, J. S. Evans, M. Fnais, D. Giannadaki, and A. Pozzer, "The contribution of outdoor air pollution sources to premature mortality on a global scale," *Nature*, vol. 525, no. 7569, pp. 367–371, Sep. 2015.

[2] S. Ohlwein, R. Kappeler, M. K. Joss, N. Künzli, and B. Hoffmann, "Health effects of ultrafine particles: A systematic literature review update of epidemiological evidence," *Int. J. Public Health*, vol. 64, no. 4, pp. 547–559, May 2019.

[3] *Who Global Air Quality Guidelines: Particulate Matter ($PM_{2.5}$ and PM_{10}), Ozone, Nitrogen Dioxide, Sulfur Dioxide and Carbon Monoxide*, World Health Org., Geneva, Switzerland, 2021.

[4] J. Andersson, B. Giechaskiel, R. M. Bueno, E. Sandbach, and P. Dilara, "Particle measurement programme (PMP) light-duty inter-laboratory correlation exercise (ILCE_LD) final report," JRC Publications Repository, TP, JRC, Ispra, Italy, Tech. Rep. EUR 22775 EN, 2007.

[5] *Ambient Air—Determination of the Particle Number Concentration of Atmospheric Aerosol*, Standard CEN/TS 16976:2016, CEN, 2016.

[6] B. Giechaskiel et al., "Review of motor vehicle particulate emissions sampling and measurement: From smoke and filter mass to particle number," *J. Aerosol Sci.*, vol. 67, pp. 48–86, Jan. 2014.

[7] S. Dhaniyala, M. Fierz, J. Keskinen, and M. Marjamäki, "Instruments based on electrical detection of aerosols," in *Aerosol Measurement: Principles, Techniques, and Applications*, 3rd ed., P. Kulkarni, P. A. Baron, and K. Willeke, Eds. Hoboken, NJ, USA: Wiley, 2011, pp. 393–416.

[8] B. Giechaskiel et al., "Inter-laboratory correlation exercise with portable emissions measurement systems (PEMS) on chassis dynamometers," *Appl. Sci.*, vol. 8, no. 11, p. 2275, Nov. 2018.

[9] A. Melas, T. Selleri, R. Suarez-Bertoa, and B. Giechaskiel, "Evaluation of solid particle number sensors for periodic technical inspection of passenger cars," *Sensors*, vol. 21, no. 24, p. 8325, Dec. 2021.

[10] L. Ntziachristos, B. Giechaskiel, J. Ristimäki, and J. Keskinen, "Use of a corona charger for the characterisation of automotive exhaust aerosol," *J. Aerosol Sci.*, vol. 35, no. 8, pp. 943–963, Aug. 2004.

[11] A. Rostedt et al., "Non-collecting electrical sensor for particle concentration measurement," *Aerosol Air Quality Res.*, vol. 9, no. 4, pp. 470–477, 2009.

[12] S. Amanatidis, M. M. Maricq, L. Ntziachristos, and Z. Samaras, "Measuring number, mass, and size of exhaust particles with diffusion chargers: The dual Pegasor Particle Sensor," *J. Aerosol Sci.*, vol. 92, pp. 1–15, Feb. 2016.

[13] M. A. Schriefl, A. Bergmann, and M. Fierz, "Design principles for sensing particle number concentration and mean particle size with unipolar diffusion charging," *IEEE Sensors J.*, vol. 19, no. 4, pp. 1392–1399, Feb. 2019.

[14] P. Karjalainen et al., "Fuel-operated auxiliary heaters are a major additional source of vehicular particulate emissions in cold regions," *Atmosphere*, vol. 12, no. 9, p. 1105, Aug. 2021.

[15] A. Melas, K. Vasilatou, R. Suarez-Bertoa, and B. Giechaskiel, "Laboratory measurements with solid particle number instruments designed for periodic technical inspection (PTI) of vehicles," *Measurement*, vol. 215, Jun. 2023, Art. no. 112839.

[16] K. Vasilatou et al., "Effects of the test aerosol on the performance of periodic technical inspection particle counters," *J. Aerosol Sci.*, vol. 172, Aug. 2023, Art. no. 106182.

[17] J. Marra, W. van den Brink, H. Goossens, and S. Kessels, "Nanoparticle monitoring for exposure assessment," *IEEE Nanotechnol. Mag.*, vol. 3, no. 2, pp. 6–37, Jun. 2009.

[18] M. Fierz, C. Houle, P. Steigmeier, and H. Burtscher, "Design, calibration, and field performance of a miniature diffusion size classifier," *Aerosol Sci. Technol.*, vol. 45, no. 1, pp. 1–10, Jan. 2011.

[19] W. C. Hinds, *Aerosol Technology: Properties, Behavior, and Measurement of Airborne Particles*, 2nd ed. Hoboken, NJ, USA: Wiley, 1999.

[20] E. A. Mason and E. W. McDaniel, *Transport Properties of Ions in Gases*. Hoboken, NJ, USA: Wiley, 1988.

[21] F. W. Peek, *Dielectric Phenomena in High Voltage Engineering*, 3rd ed. New York, NY, USA: McGraw-Hill, 1929.

[22] P. G. Gormley and M. Kennedy, "Diffusion from a stream flowing through a cylindrical tube," *Proc. Roy. Irish Acad. A, Math. Phys. Sci.*, vol. 52, pp. 163–169, Jan. 1948.

[23] M. D. Allen and O. G. Raabe, "Slip correction measurements of spherical solid aerosol particles in an improved Millikan apparatus," *Aerosol Sci. Technol.*, vol. 4, no. 3, pp. 269–286, Jan. 1985.

[24] J. Yli-Ojanperä, J. M. Mäkelä, M. Marjamäki, A. Rostedt, and J. Keskinen, "Towards traceable particle number concentration standard: Single charged aerosol reference (SCAR)," *J. Aerosol Sci.*, vol. 41, no. 8, pp. 719–728, Aug. 2010.

[25] M. Marjamäki, J. Keskinen, D.-R. Chen, and D. Y. H. Pui, "Performance evaluation of the electrical low-pressure impactor (ELPI)," *J. Aerosol Sci.*, vol. 31, no. 2, pp. 249–261, Feb. 2000.

[26] H. Oh, H. Park, and S. Kim, "Effects of particle shape on the unipolar diffusion charging of nonspherical particles," *Aerosol Sci. Technol.*, vol. 38, no. 11, pp. 1045–1053, Nov. 2004.

[27] M. M. Maricq, "Bipolar diffusion charging of soot aggregates," *Aerosol Sci. Technol.*, vol. 42, no. 4, pp. 247–254, Mar. 2008.

Elmeri Laakkonen currently pursuing the M.Sc. degree with Tampere University, Tampere, Finland.

He is also currently working with Dekati Ltd., Tampere, as an Aerosol Measurement Specialist.

Anssi Arffman received the M.Sc. and Ph.D. degrees from Tampere University of Technology on Aerosol Physics, Tampere, Finland, in 2009 and 2016, respectively.

He is currently a Technology Manager and a Scientist with Dekati Ltd., Tampere.

Antti Rostedt is a Staff Scientist with the Aerosol Physics Laboratory, Faculty of Engineering and Natural Sciences, Tampere University, Tampere, Finland. His main research interests include aerosol measurement technology and instrument development.

Jorma Keskinen is the Head of the Aerosol Physics Laboratory, Faculty of Engineering and Natural Sciences, Tampere University, Tampere, Finland. His research interests include aerosol measurement techniques, emissions of engines, vehicles, and ships—especially nanoparticles, volatility, and secondary aerosol formation potential.